Acta Geotechnica
https://doi.org/10.1007/s11440-024-02388-8

RESEARCH PAPER

Assessing the reuse of liquid nitrogen in artificial ground freezing through field experiments

Hyun-Jun Choi[1] · Seokjae Lee[2] · Hyobum Lee[3] · Sangyeong Park[4,6] · Hangseok Choi[4] · Jongmuk Won[5]

Received: 16 October 2022 / Accepted: 11 August 2024

Abstract

Liquid nitrogen is the most common refrigerant adopted in the artificial ground freezing (AGF) method for the rapid freezing of soil. However, the relatively high price of liquid nitrogen demands the reuse of liquid nitrogen in AGF, which utilizes partially gasified liquid nitrogen after an initial injection. This study investigated the reusability of liquid nitrogen in AGF by performing a field experiment. Temperatures of the ground were monitored near the sub-freezing pipes installed 1 m away from the main freezing pipes, where liquid nitrogen was initially injected. A frozen wall having a thickness of 1 m was formed between two sub-freezing pipes after 5 days of injecting liquid nitrogen into the main freezing pipes. Furthermore, the lowest temperature of − 12 °C measured in the sub-freezing pipe implied that the temperature of nitrogen after circulating through the main freezing pipe was sufficiently low to freeze the surrounding soil formation. The freezing rate, elapsed time for freezing, and freezing duration evaluated from the monitored temperature data also demonstrated the promising potential of reusing liquid nitrogen in AGF for saturated silty deposits.

Keywords Artificial ground freezing · Field experiment · Frozen wall · Liquid nitrogen · Reuse

Abbreviations

AGF	Artificial ground freezing
SPT	Standard penetration test
LL	Liquid limit
PI	Plasticity index
USCS	Unified soil classification system

✉ Jongmuk Won
jwon@unist.ac.kr

[1] Northern Infrastructure Specialized Team, Korea Institute of Civil Engineering and Building Technology, 283 Goyangdae-Ro, Ilsanseo-Gu, Goyang 10223, South Korea

[2] Department of Civil Engineering, Kunsan National University, 558 Daehak-ro, Gunsan, 54150, South Korea

[3] Advanced Railroad Civil Engineering Division, Korea Railroad Research Institute, 176 Railroad Museum Road, Uiwang-si, Gyeonggi-do 16105, South Korea

[4] School of Civil, Environmental and Architectural Engineering, Korea University, 145 Anam-ro, Seoul 02841, South Korea

[5] Department of Civil, Urban, Earth, and Environmental Engineering, Ulsan National Institute of Science and Technology, 50 UNIST-gil, Ulsan 44919, South Korea

[6] Harold Vance Department of Petroleum Engineering, Texas A&M University, 400 Bizzell Street, Texas 77840 College Station, USA

1 Introduction

For the past few decades, the artificial ground freezing (AGF) method has been widely adopted as an eco-friendly temporary ground support technique in various engineering projects, such as tunnel excavation [12, 23, 28, 30, 35, 38, 40], mining [45], and containment of hazardous wastes [3, 6]. Frozen soil can be formed by heat transfer from the soil to freezing pipes. This increases the stiffness or strength and decreases the hydraulic conductivity of soil [2, 5, 18, 21, 36]. Brine and liquid nitrogen are the two most commonly used refrigerants in AGF, which extract the heat energy of the ground while circulating through the freezing pipe. Because of the vaporization characteristics of liquid nitrogen after heat extraction, AGF by injecting liquid nitrogen is called an open system, whereas AGF by circulating brine is called a closed system [38, 46].

The low boiling point (− 196 °C) of liquid nitrogen freezes the surrounding soil faster than brine, which has a higher temperature (− 40 to − 20 °C) during circulation. However, because liquid nitrogen is typically not reusable,

Published online: 18 September 2024

the open system is more expensive than the closed system for achieving a target volume of frozen soil. Therefore, a hybrid method, combining open and closed systems, is occasionally employed to form a frozen wall quickly using the open system (typically within a few days), followed by maintaining the frozen wall for a relatively long period using the closed system (lasting several months) [32, 39, 40]. The hybrid method, which may provide a significant economic benefit over the open system itself, combines the advantages of the two freezing systems [50].

For the effective performance of the hybrid method, the initial formation of the frozen soil by injecting liquid nitrogen is critical. Therefore, the formation of frozen walls by injecting liquid nitrogen under various thermal and hydraulic conditions was investigated to provide insights into the effective implementation of AGF under such conditions [20, 23, 26, 27, 34, 48].

The economic constraint of liquid nitrogen may be compensated by circulating liquid nitrogen in the two freezing pipes instead of releasing the partially gasified liquid nitrogen after an initial injection. This scenario can be achieved when the liquid nitrogen is only partially gasified, indicating that it still holds significant potential to extract heat from the ground during the second injection. The opportunity to reuse partially gasified liquid nitrogen can be enhanced when the freezing pipe is positioned at a relatively shallow depth. Although this approach is feasible in practical applications, the potential for reusing liquid nitrogen in AGF has not been thoroughly documented. Therefore, the objective of this study is to investigate the applicability of reusing liquid nitrogen through a field experiment. The efficiency of the reused liquid nitrogen after the initial circulation was assessed based on the observed temperature near the sub-freezing pipes during the second injection. The elapsed time for freezing and the freezing duration obtained from the temperature data were evaluated to quantitatively describe the reusability of liquid nitrogen in AGF.

2 Experimental program

2.1 Testbed description

The AGF field experiment was performed in Ganghwa-gun, Incheon, Republic of Korea, 600 m from the Yellow Sea (Fig. 1a). To obtain the comprehensive geological profile of the testbed, boring and standard penetration tests (SPTs) were conducted at three locations, each located 10 m apart from the freezing pipes, as shown in Fig. 1b, c. Boring was performed up to a depth of 10 m using an NX-core-sized hole with an outer diameter of 76 mm. The geological profiles of the three boreholes, along with N values measured at every 1 m depth, are shown in Fig. 1b. In this figure, the SPT-N values are presented with depth, expressed as blow counts per penetration depth of 300 mm.

The site investigations revealed a surface fill layer composed of clayey silt from the surface to the depth of 1 m. Additionally, the sedimentary layer, mostly composed of clayey silt, was located below the fill layer (Fig. 1b). The soil layer from the surface to the depth of 5 m (where the freezing pipes were installed) was classified as very soft or soft ground by the SPT-N values of 1–7. The groundwater level was determined during the boring process by measuring the distance between the ground surface and the water level in the boreholes. It was observed that the groundwater levels were almost similar, at 2 m, in all three boreholes (see GWL in Fig. 1b). This observation suggests a static condition of the groundwater in the testbed, indicating minimal or no water flow.

Laboratory tests were performed on the undisturbed samples obtained from the borehole BH-2 to evaluate the soil properties of the testbed (Table 1). The salinity of the pore water was measured because the test bed was adjacent to the sea. However, the salinity of the testbed across all depths (2–10 m) was approximately 0, indicating that the effect of salinity on ground freezing was negligible (since an increase in salinity lowers the freezing point of pore water [8]). This also suggests that the salt water wedge did not affect the experimental results, as the freezing pipes were installed up to a depth of 5 m in this study. The water content range was 22.6–36.7%, and most of the soil samples passed the #200 sieve (opening size of 75 μm). From the measured liquid limit (LL) and plasticity index (PI), all samples were classified as ML (silt with low plasticity) in accordance with the unified soil classification system (USCS). However, the sample obtained at the depth interval of 0–0.8 m was classified as CL (clay with high plasticity).

The thermal conductivity of soil affects the ground freezing rate significantly [37]. Previous experimental and theoretical studies have documented that the thermal conductivity of frozen soils is approximately twice that of unfrozen soils [17, 25]. This implies that heat conduction from the freezing pipe to the soil near the freezing pipe becomes faster as the freezing front propagates. To investigate the thermal characteristics at the testbed, the thermal conductivities of the unfrozen and frozen soils were measured using QTM-500 (Kyoto Electronics) by adopting the transient hot-wire method. The sampled clayey silt was placed in a mold (100 (length) × 50 (width) × 20 (height) mm) to measure the thermal conductivity of the sample using a QTM-500 (Kyoto Electronics Manufacturing Co., Ltd.) equipped with a 95 × 40 mm flat probe. The thermal conductivity of the unfrozen soil was measured in the laboratory at an ambient

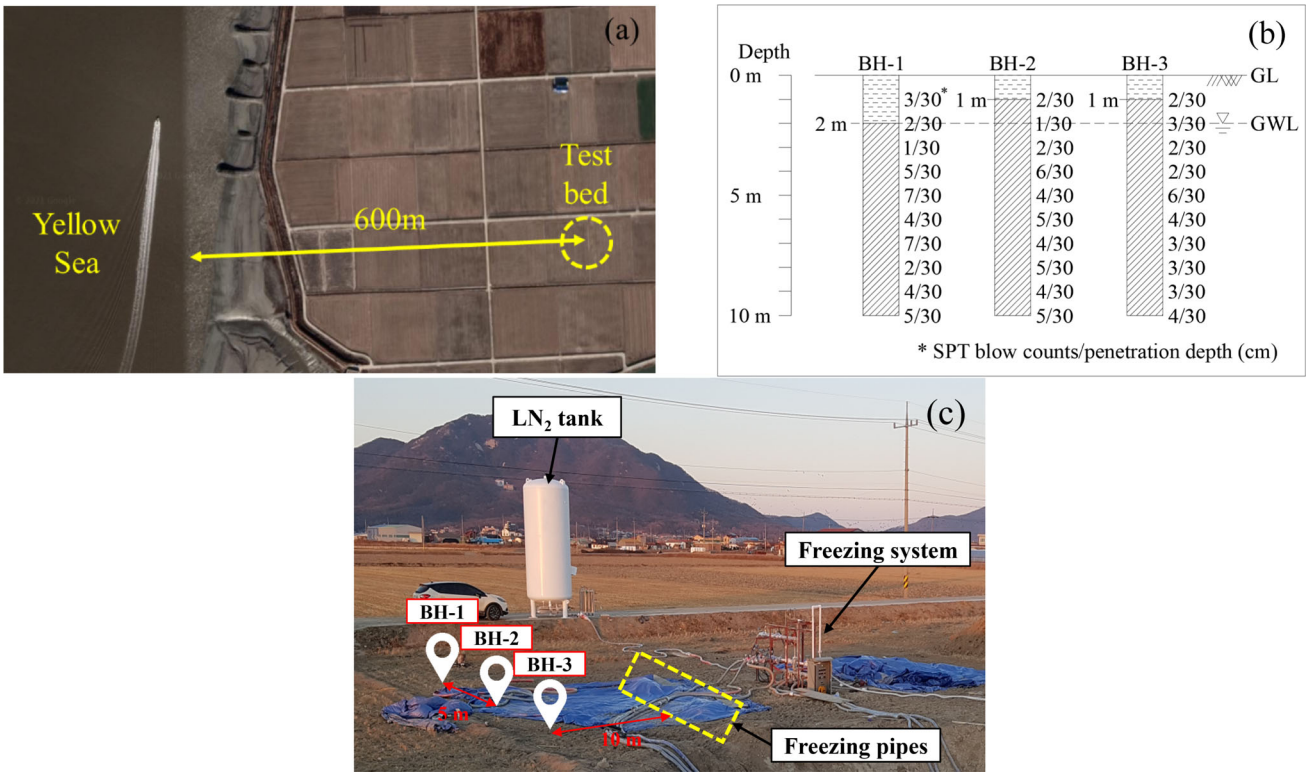

Fig. 1 Plan view and geologic profile of the testbed

Table 1 Soil properties of testbed obtained from undisturbed samples

Depth (m)	Dry unit weight (g/cm^3)	Water content (%)	Salinity (%)	Grain size analysis % finer than			Atterberg limits		USCS
				425 μm (#40)	75 μm (#200)	2 μm*	LL (%)	PI (%)	
0–0.8	1.219	22.6	0.0	100	99.0	18.3	42.6	18.5	CL
1.0–1.8	1.228	27.4		100	99.2	15.9	41.1	14.8	ML
2.0–2.8	1.225	42.2		100	99.5	12.8	45.1	17.2	ML
3.0–3.8	1.242	41.5		100	99.4	6.4	39.8	9.6	ML
4.0–4.8	1.267	36.0		100	98.0	4.0	33.9	5.7	ML
5.0–5.8	1.253	36.7		100	98.7	3.7	31.4	4.2	ML

*Measured via the hydrometer test (ASTM D422)

Table 2 Thermal conductivity of unfrozen and frozen soils at the testbed

Depth (m)	Thermal conductivity (W/mK)	
	Unfrozen (15 °C)	Frozen (− 10 °C)
1.0–1.8	1.088	1.905
2.0–2.8	1.133	2.525
3.0–3.8	1.208	2.388
4.0–4.8	1.077	2.282
5.0–5.8	1.147	2.077

temperature of 15 °C. As for the frozen soil, the specimens in the mold were placed in a freezer at − 10 °C for 24 h before measuring the thermal conductivity. The preliminary result ensured the freezing of the entire specimen at a temperature lower than 0 °C when the specimen was placed in the freezer for more than 10 h. To minimize the thawing effect on measuring thermal conductivity, the model and probe were placed in a freezer during the measurement. Table 2 shows the measured thermal conductivities of the unfrozen and frozen testbed soils. Note that the higher thermal conductivity of frozen soils than that of unfrozen soils, presented in Table 2, is consistent with the results presented in the literature [7, 37, 43].

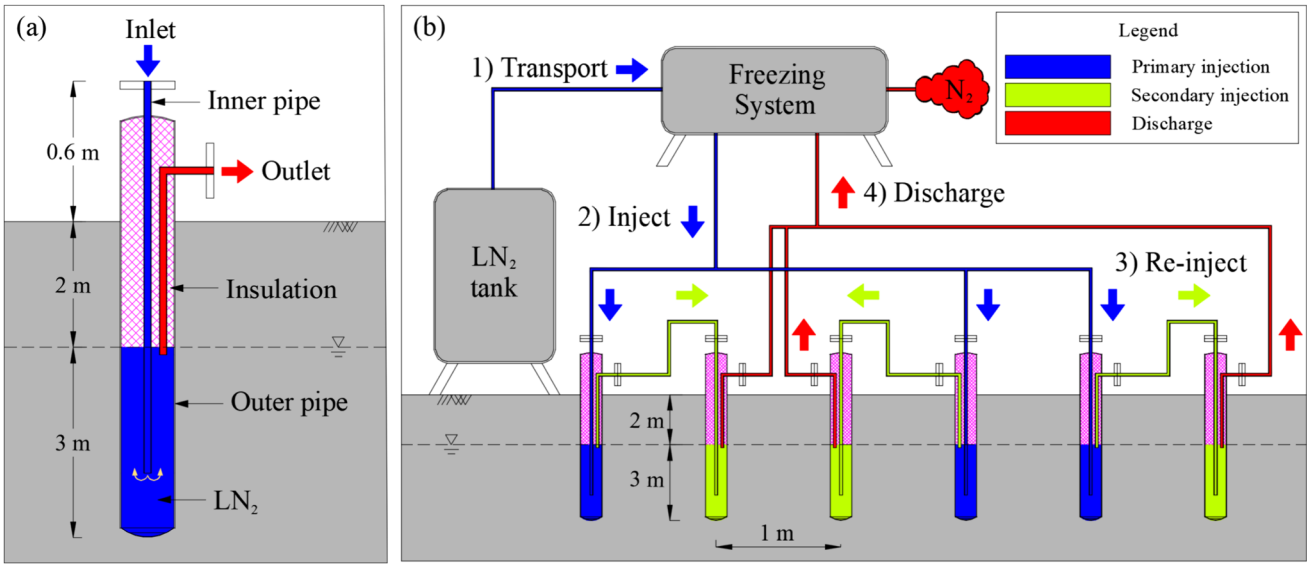

Fig. 2 Configuration of freezing pipes and flow of liquid nitrogen in the field experiment

2.2 Overview of application of recycled liquid nitrogen

The liquid nitrogen stored in a storage tank was injected into three freezing pipes (named as the main freezing pipes) installed up to 5 m deep to extract heat from the ground through the freezing pipes. To investigate the reusability of liquid nitrogen, the outlet of the main freezing pipes was connected to the adjacent freezing pipes with the identical dimensions (referred to as the sub-freezing pipes in this study) installed 1 m away from the main freezing pipes (Fig. 2b). Then, the second heat extraction was induced through the sub-freezing pipes, followed by releasing gasified nitrogen after the second heat extraction.

The distance between the freezing pipes (1 m) was consistent to form a typical target thickness of the frozen wall employed in AGF [14, 24, 29]. The length and diameter of the outer freezing pipe were 5.2 m and 89.1 mm, and those of the inner freezing pipe were 5.3 m and 21.7 mm, respectively. Because ground freezing involves a phase change process from pore water to ice, the characteristics of ground freezing, such as freezing rate, vary depending on the degree of saturation and groundwater flow [10, 11, 19]. To freeze the saturated soil below the groundwater table (2 m), the freezing pipe was thermally insulated up to the depth of 2 m from the ground surface (Fig. 2a).

As shown in Fig. 2b, the injection of liquid nitrogen was divided into four steps. (1) The liquid nitrogen stored in the tank was transported to the freezing system to control the flow rate of liquid nitrogen. (2) The liquid nitrogen was injected into the three main freezing pipes with an injection pressure of ~ 5 bar for primary heat extraction. (3) The liquid nitrogen from the main freezing pipes was re-injected into the sub-freezing pipes for additional heat extraction. (4) The gasified nitrogen was discharged into the atmosphere.

To monitor temperature changes during the injection of liquid nitrogen, 33 temperature-measuring holes were installed at 0.25 m intervals near the freezing pipes (Fig. 3). Thermocouples were installed at every 0.5 m between the depth of 1.5–6.0 m in the temperature-measuring holes and 0.5–5.0 m in the freezing pipes. The discharge temperature of nitrogen after the secondary injection remained constant through the automatic valve installed in the freezing system at approximately − 120 °C. The automatic valve was closed when the discharge temperature of nitrogen dropped below − 120 °C to ensure sufficient heat extraction from the ground. When the discharge temperature exceeded − 120 °C after sufficient heat extraction, the valve opened automatically and liquid nitrogen was injected into the freezing pipe. Note that the configuration of temperature-measuring holes was selected to monitor the formation of a frozen wall with a thickness of 1 m.

The arrangement of the temperature-measuring holes can be divided into two groups, as shown in Fig. 4. Frozen soil was formed by a single main freezing pipe (main only in Fig. 3). A single sub-freezing pipe (sub-only in Fig. 3) at both ends of the layout, as illustrated in Fig. 3, were selected as the first group (Fig. 4a). The second group represented the formation of a frozen wall between two adjacent freezing pipes. The temperature evolution at the temperature-measuring holes for the following three scenarios was investigated: freezing between the two main freezing pipes, freezing between the two sub-freezing pipes, and freezing between the main and sub-freezing

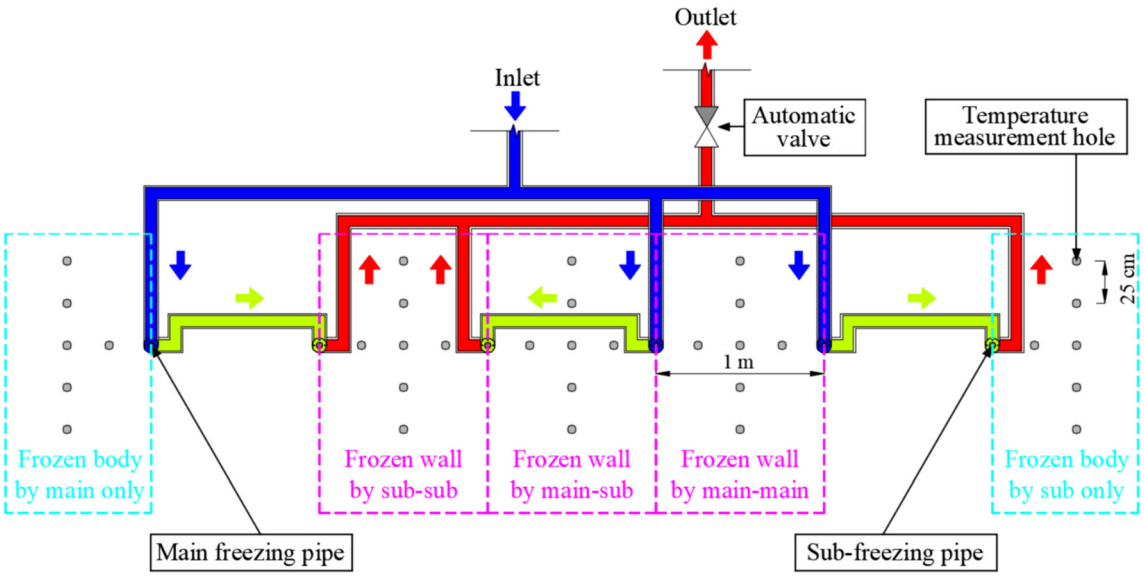

Fig. 3 Schematic of the freezing system for injecting and discharging liquid nitrogen

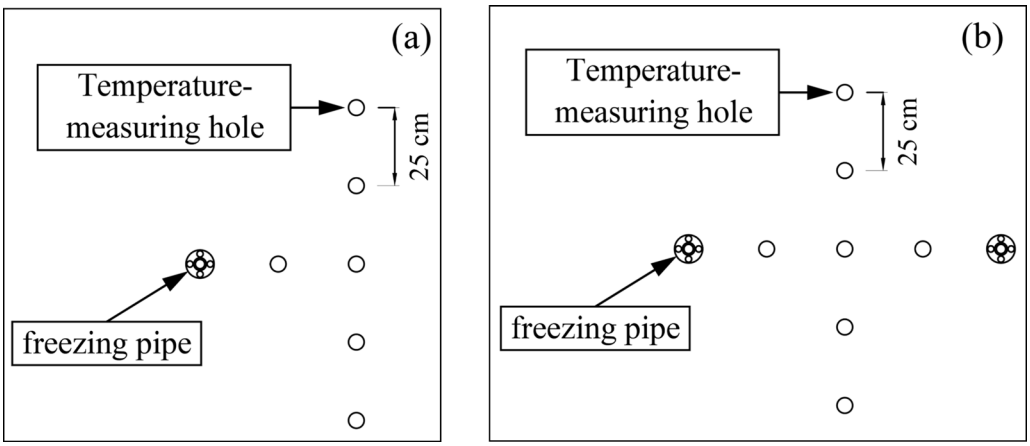

Fig. 4 Arrangement of freezing pipes and temperature-measuring holes. **a** Freezing near the single freezing pipe (first group) and **b** freezing between two freezing pipes (second group)

pipes. To monitor the temperature evolution and freezing time of the ground for the two groups, the distance between the six freezing pipes was 1 m, and the distances between the freezing pipes and temperature-measuring holes were 25, 50, 55.9, and 70.7 cm (Fig. 3). Liquid nitrogen was injected for 5 days (120 h) while maintaining the discharge temperature of − 120 °C.

3 Experimental program

3.1 Monitored temperature at temperature-measuring holes

During the field experiment, a liquid nitrogen tank having a capacity of 16 tons was recharged twice a day. A total of 32.364 tons of liquid nitrogen was consumed under 5 bars for 5 days. The daily consumption of liquid nitrogen is presented in Table 3.

Table 3 Liquid nitrogen consumption

Elapsed day (days)	Injection rate (ton/day)	Cumulative weight (tons)
1	7.089	7.089
2	7.537	14.626
3	7.249	21.875
4	5.314	27.189
5	5.175	32.364
Average	6.473	–

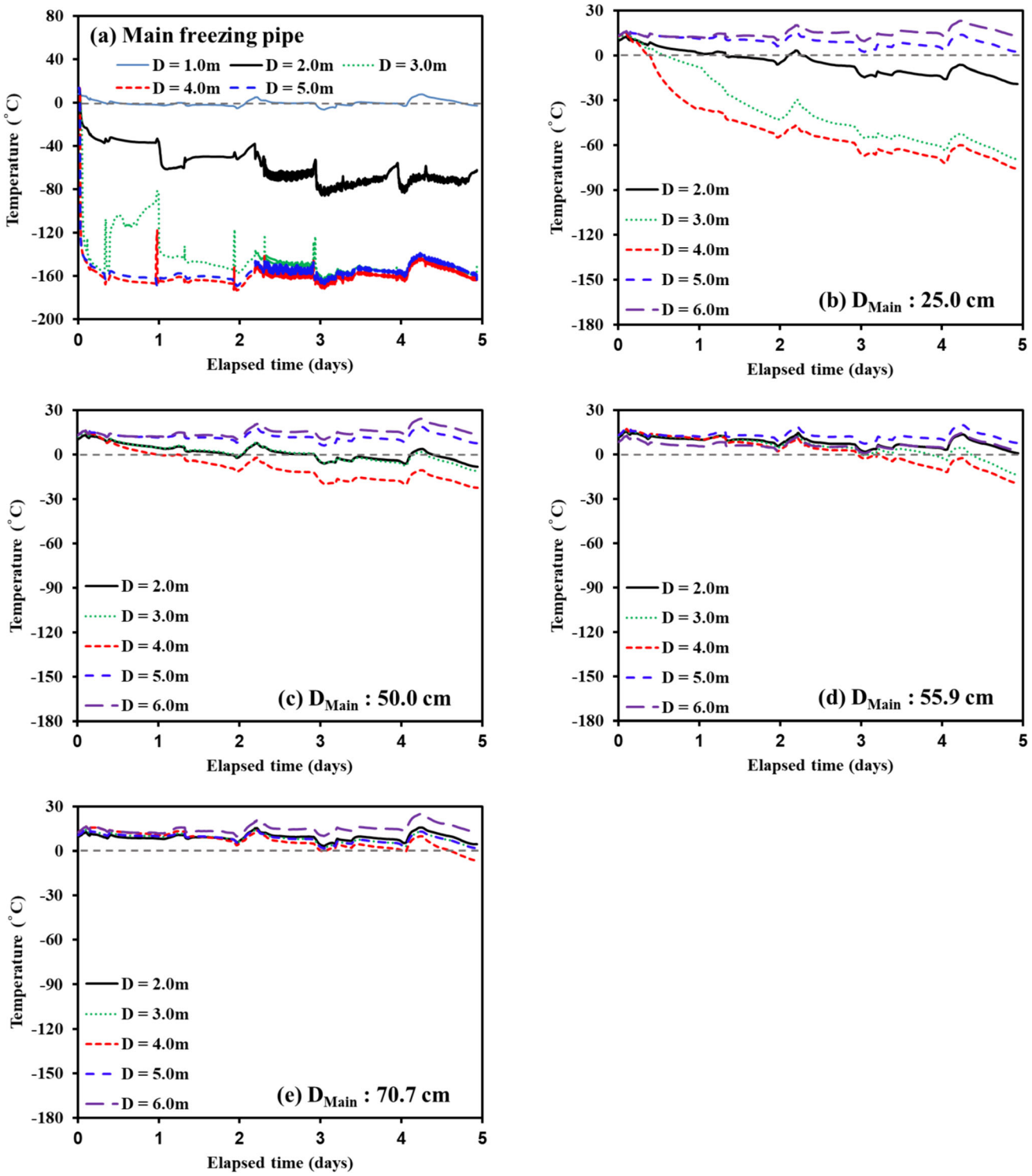

Fig. 5 Temperature evolution during injection of liquid nitrogen for single main freezing pipe. **a** Main freezing pipe; At **b** 25 cm; **c** 50 cm; **d** 55.9 cm; and **e** 70.7 cm from freezing pipe

Figures 5, 6, 7, 8, and 9 illustrate the evolution of temperature at the freezing pipe outer wall and the ground during the injection of liquid nitrogen for the five scenarios. The main freezing pipe only (Fig. 5), sub-freezing pipe only (Fig. 6), two main freezing pipes (Fig. 7), two sub-freezing pipes (Fig. 8), and main and sub-freezing pipes (Fig. 9) are denoted as main-only setup, sub-only setup, main-main setup, sub-sub setup, and main-sub setup,

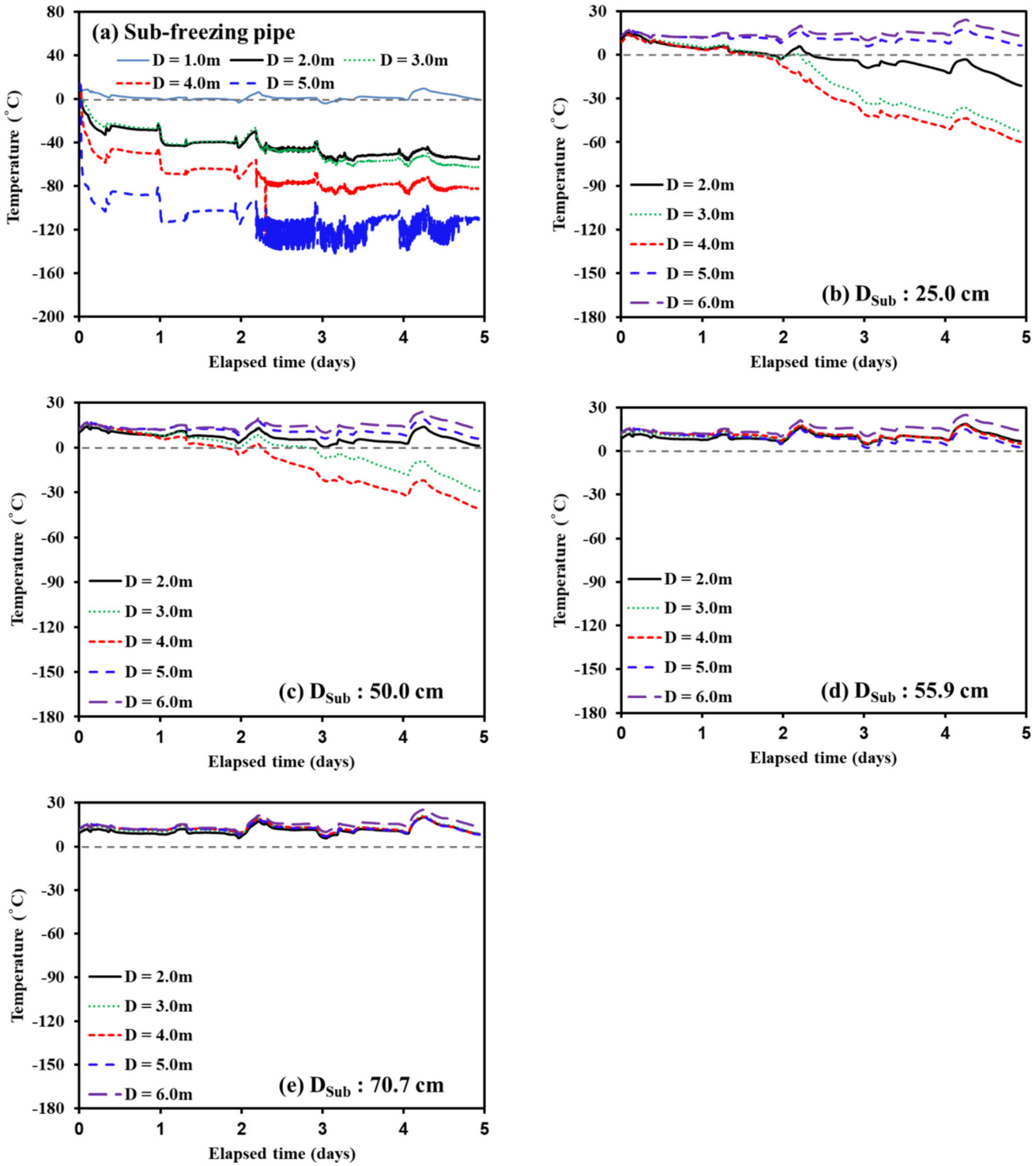

Fig. 6 Temperature evolution during injection of liquid nitrogen for single sub-freezing pipe. **a** Sub-freezing pipe; At **b** 25 cm, **c** 50 cm, **d** 55.9 cm, and **e** 70.7 cm from freezing pipe

respectively, in the following text. As shown in Figs. 5a, 7a, b, and 9a, the temperatures measured at the outer walls of the freezing pipes at depths of 4 and 5 m were relatively consistent during the injection, whereas a higher temperature at the depth of 3 m than at depths of 4 and 5 m was observed for the first two days. The temperature at the depth of 3 m was consistent with that at the depths of 4 and 5 m after the elapsed time greater than 2 days. This indicates significant heat extraction in the middle of the main freezing pipes during the formation of frozen soil near the

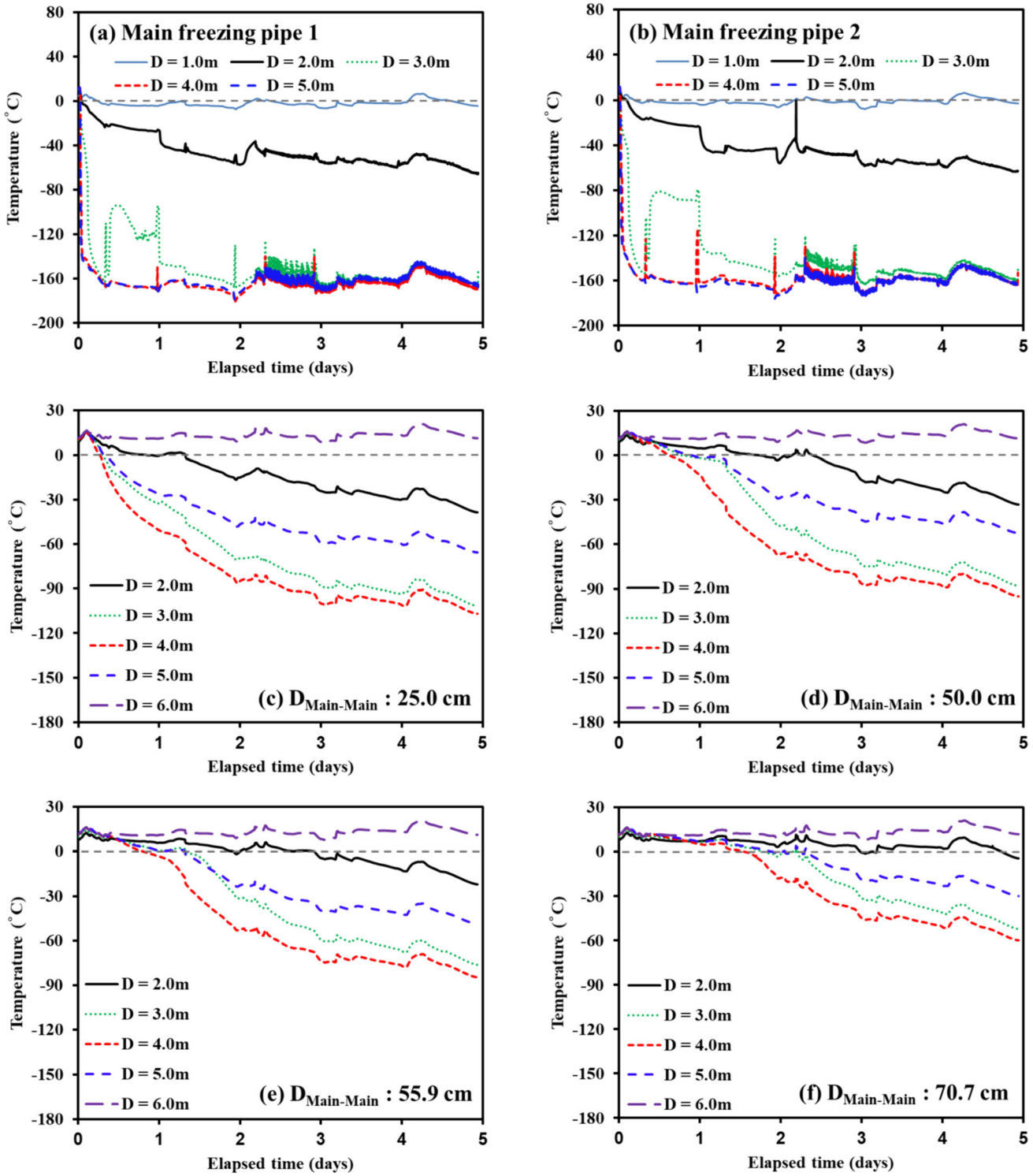

Fig. 7 Temperature evolution during injection of liquid nitrogen for two main freezing pipes. **a** Main freezing pipe 1; **b** Main freezing pipe 2; At **c** 25 cm, **d** 50 cm, **e** 55.9 cm, and **f** 70.7 cm from freezing pipe

freezing pipes. A consistent temperature after 2 days at the depths of 3, 4, and 5 m implies an identical rate of heat extraction. This occurred after a certain volume of soil froze near the freezing pipe. Additionally, the relatively low temperature of − 120 °C at the depth of 5 m in the sub-freezing pipe indicates the possibility of partially gasified liquid nitrogen after the initial circulation. Although liquid nitrogen was completely gasified in the

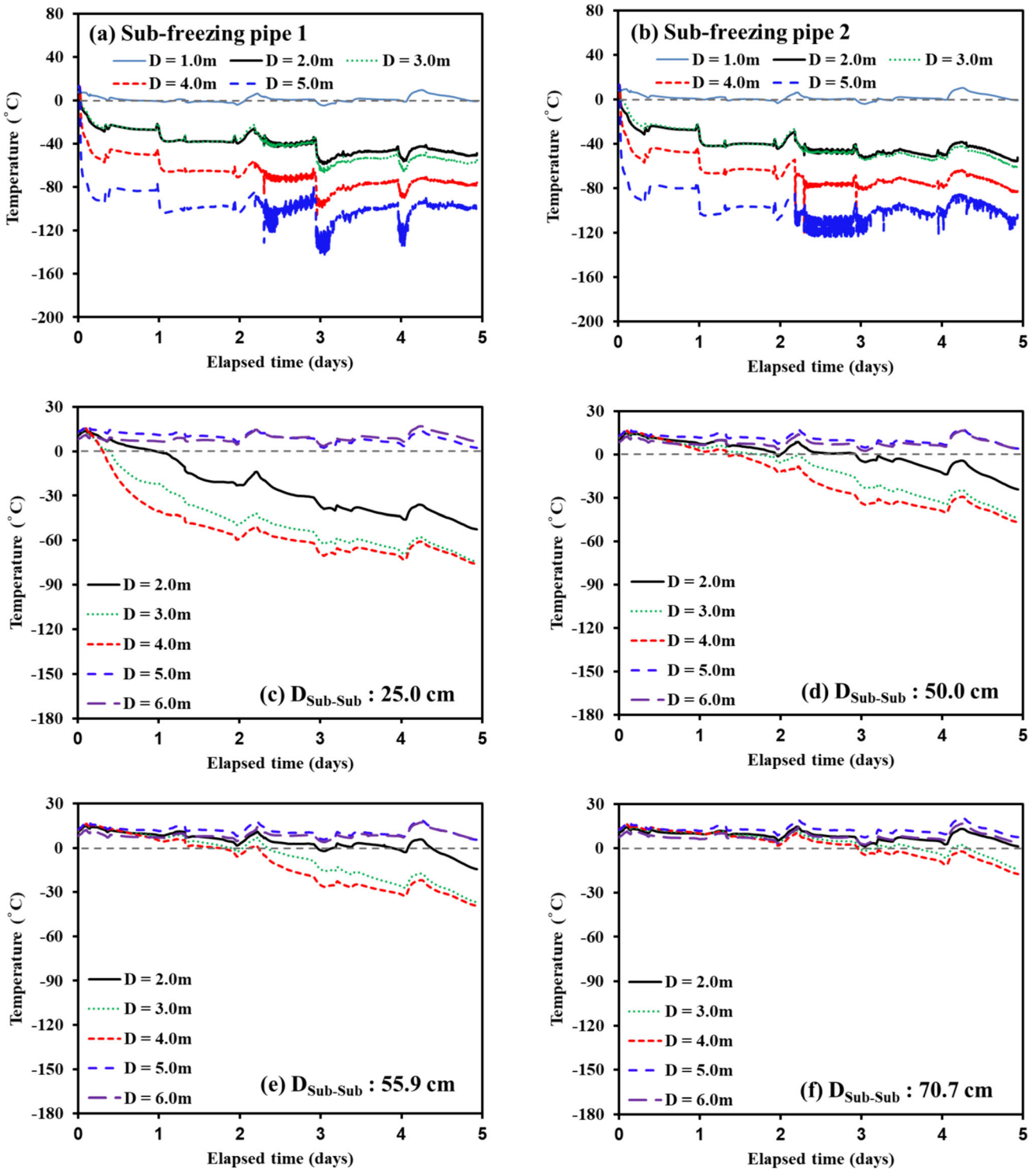

Fig. 8 Temperature evolution during injection of liquid nitrogen for two sub-freezing pipes. **a** Sub-freezing pipe 1; **b** Sub-freezing pipe 2; At **c** 25 cm, **d** 50 cm, **e** 55.9 cm, and **f** 70.7 cm from freezing pipe

sub-freezing pipe, − 120 °C might be sufficient to freeze the soil near the sub-freezing pipe.

It should be noted that the phase of liquid nitrogen in the freezing pipe was not directly identified in this study. However, the high injection pressure of 5 bar applied into the main freezing pipes and the lower monitored temperature at shallower depths in the sub-freezing pipes indicate the boiling point of liquid nitrogen under high pressure and

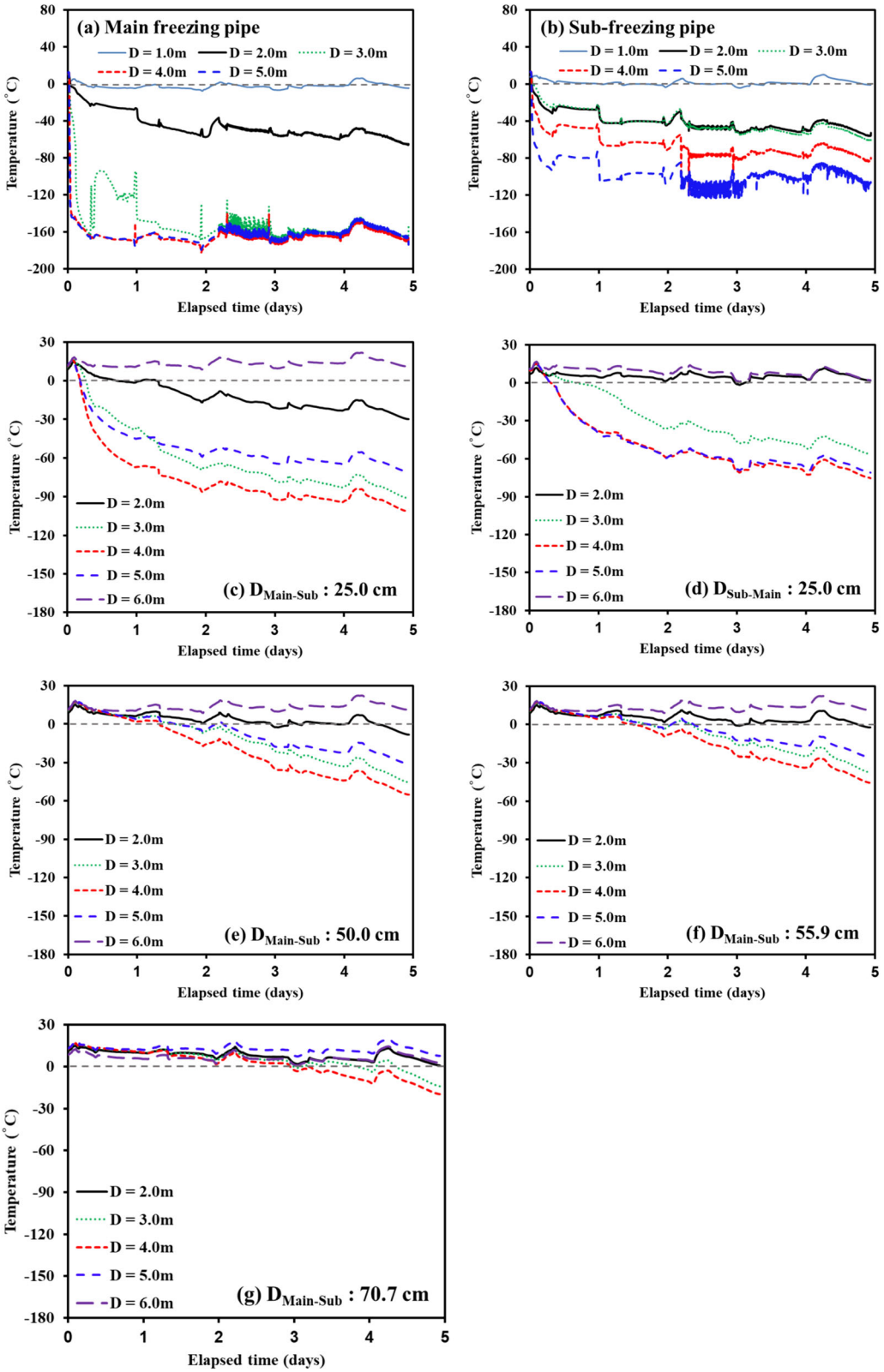

Fig. 9 Temperature evolution during injection of liquid nitrogen between main freezing pipe and sub-freezing pipe. **a** Main freezing pipe; **b** Sub-freezing pipe; At **c** 25 cm from main freezing pipe, **d** 25 cm from sub-freezing pipe, **e** 50 cm from freezing pipe, **f** 55.9 cm from freezing pipe, and **g** 70.7 cm from freezing pipe

the occurrence of heat extraction in the sub-freezing pipes. This implies that the liquid nitrogen was likely partially gasified after the initial injection. Additionally, it is worth mentioning that the temperature of liquid nitrogen in the freezing pipes was likely lower than the monitored temperature because the thermocouples were attached to the outside of the freezing pipes. Because heat extraction was initiated at the bottom of the freezing pipe when the injected liquid nitrogen flowed upward through the outer freezing pipe (Fig. 2a), the monitored temperature data at the main and sub-freezing pipes were in the order of depth of 1 m > 2 m > 3 m > 4 m > 5 m.

In all temperature-measuring holes, the dominant heat extraction from the soil occurred in the radial direction (refer to Figs. 5, 6, 7, 8, and 9). The dominant heat extraction from the soil occurred in the radial direction. Additionally, the lowest temperature was observed at the depth of 4 m, implying that the semi-spherical shape of the frozen soil near the freezing pipe was formed with a maximum radial distance at the depth of 4 m. For the first group (main-only and sub-only setups), an above-zero temperature at the depth of 5 m at the distance of 25 cm (Figs. 5b and 6b) indicates that heat conduction from the ground temperature below 5 m impeded the radial formation of frozen soil at the depth of 5 m.

The temperature corresponding to the elapsed time of 5 days at the depth of 4 m for D = 25 cm was in the order of sub-only setup (Fig. 6b) > main-only setup (Fig. 5b) ≈ sub-sub setup (Fig. 8c) > main-sub setup (Fig. 9c) > main-main setup (Fig. 7c). This indicates that the most rapid and slowest heat extraction and formation of frozen soil occurs in the main-main setup and sub-freezing pipe only cases, respectively. Similar temperature values (approximately − 76 °C) at the distance of 25 cm for the cases of main-only and sub-sub setups indicate that the evolution of frozen soil between the two freezing pipes with the circulation of reused liquid nitrogen may have similar performance in freezing soils at a relatively short distance (25 cm) from the freezing pipe. On the other hand, lower temperatures were observed for the sub-sub setup (Fig. 8d, e, f) than those for the main-only setup (Fig. 5c, d, e) at the distances of 50, 55.9, and 70.7 cm. This suggests a higher freezing efficiency for the sub-sub setup than the main-only setup at these specific distances. The observed below-zero temperature at the distance of 50 cm for sub-only setup (Fig. 6c) implies that liquid nitrogen can be reused within a 3 m depth interval (heat extraction from 2 to 5 m) between the freezing pipe and surrounding soil at a flow rate of 6.473 ton/day (Table 3). The chance of efficient reuse can be increased at a high flow rate and short depth interval of heat extraction.

3.2 Freezing rate from the experimental observations

The freezing rate of the soil was evaluated using Eq. (1) for a quantitative representation of the temperature measurements presented in Figs. 5, 6, 7, 8 and 9. Here, the freezing pipe was assumed to be an infinite line heat source, where the formation of a cylindrical frozen body surrounding the freezing pipe was anticipated. The radius of the cylindrical frozen body increases during refrigerant injection, and the freezing rate in the radial direction can be defined as the one-dimensional freezing rate of the ground [13]. The one-dimensional freezing rate of the ground (v_f (L/T)) can be expressed as follows:

$$v_f = \frac{r_f}{t}, \tag{1}$$

where v_f (L/T) is the one-dimensional freezing rate in the radial direction, r_f (L) is the radius of the frozen body (distance from the freezing pipe), and t (T) is the required freezing time (time required to reach the sub-zero temperature in temperature-measuring holes). Table 4 summarizes the one-dimensional freezing rate, evaluated from the monitored temperature at the depth of 4 m (representing averaged freezing rates for a given radius of the frozen body).

Table 4 summarizes the one-dimensional freezing rate evaluated from the monitored temperature at the depth of 4 m (averaged freezing rates for a given radius of the frozen body). As shown in Table 4, the frozen soil near the

Table 4 One-dimensional freezing rate according to the freezing temperature at 4 m below the ground surface

Radius of frozen soil (distance from the freezing pipe) (cm)	v_f (cm/h)				
	Main-only setup	Sub-only setup	Main-main setup	Sub-sub setup	Main-sub setup
25.0	2.60	0.63	3.8	3.3	5.6 (from main side)/3.1 (from sub-side)
50.0	1.99	1.14	3.2	1.5	1.6
55.9	0.79	N/A	2.8	1.3	1.5
70.7	0.63	N/A	1.8	1.0	1.0

single main freezing pipe had a radius larger than 70.7 cm, whereas that formed by the single sub-freezing pipe was less than 55.9 cm. This can be attributed to the different temperatures at the freezing pipes between main-only setup (− 160 °C) and sub-only setup (− 80 °C) (Figs. 5a, 6a). Additionally, a value of v_f for main-only corresponding to the distance of 50 cm higher by 1.74 times than that for sub-only indicates a higher heat extraction rate resulting from the lower temperature at the freezing pipe. Similar to the cases of single freezing pipes (main-only and sub-only setups), the case of main-main setup showed higher v_f than the sub-sub and main-sub setups for all radii of frozen soil because of the lower temperature at the freezing pipe. For the main-sub setup, a higher value of v_f in the main freezing pipe was observed than that in the sub-freezing pipe, implying that the freezing front propagated faster from the main freezing pipe than from the sub-freezing pipe. However, the higher values of v_f for the main-sub setup than for the main-main setup at the distance of 25 cm were counter intuitive. This was most likely because the temperature-measuring hole was slightly inclined toward the freezing pipe in the case of main-sub setup.

Overall, the values of v_f decreased as the radius of frozen soil increased, except in the case of sub-only setup (Table 4). This is because the contact area between the frozen soil and unfrozen soil is proportional to the squared radius of the frozen soil. This decreases the rate of heat extraction in the radial direction. Because the temperature of the freezing pipe at the depth of 4 m was almost consistent during the experiment, the results presented in Table 4 indicate the anticipated evolution of the frozen soil near the freezing pipe. However, as the radius of the frozen soil increased, a more rapid decrease in v_f for the sub-sub setup case was observed than for the main-main setup, indicating that the v_f value is a function of temperature at the freezing pipe. The higher temperature of the freezing pipe for the sub-sub setup resulted in lower freezing efficiency after forming a certain radius of frozen soil.

Assuming the frozen soil near the freezing pipe to be circle-shaped in the plane view, the formation of a frozen wall between the two freezing pipes can be divided into four stages, as shown in Fig. 10. (1) The radius of frozen soil was 25 cm around each freezing pipe. (2) The radius of frozen soil was 50 cm where two frozen masses were first encountered. (3) The thickness of frozen wall was 50 cm. (4) The target thickness (1 m) of the frozen wall was achieved. The schematic drawings illustrated in Fig. 10 indicate the relationship between the monitored temperature and thickness of the frozen sample. For example, the monitored temperature at a distance of 70.7 cm corresponds to the thickness of the frozen wall becoming 1 m (Fig. 10d).

The observed temperatures presented in Figs. 7f, 8f, and 9g demonstrate that a 1-m-thick frozen wall was obtained at the depths of 3 and 4 m in all three scenarios (the cases of main-main, sub-sub, and main-sub setups) after 5 days of injecting liquid nitrogen. However, only the case of main-main setup could achieve a 1-m-thick frozen wall at the depth of 5 m. This implies the thickest frozen wall in the vertical direction was formed in the main-main setup. Furthermore, the observed sub-zero temperature at relatively short elapsed time at all depths for main-main setup (Fig. 7f) results in the most rapid formation of the 1-m-thick frozen wall, and a thickness greater than 1 m can be anticipated after injecting liquid nitrogen for more than 5 days.

3.3 Elapsed time for freezing

The reuse of liquid nitrogen can be assessed by evaluating the elapsed freezing time (t_e) and freezing duration (T_{fr}) from the temperature data shown in Figs. 5, 6, 7, 8 and 9. The mathematical expressions for t_e and T_{fr} are as follows:

$$t_e = t_{pn(1)} - t_s \tag{2}$$

$$T_{\mathrm{fr}} = T_T - t_{pn(1)} - \sum_i \left(t_{np(i)} - t_{pn(i)}\right), \tag{3}$$

where $t_{pn(i)}$ is the ith time at which the measured temperature changed to sub-zero, t_s is the starting time of liquid nitrogen injection (0 in this study), T_T is the overall time (5 days in this study), and $t_{np(i)}$ is the ith time at which the measured temperature changed back to above zero.

The evaluated t_e and T_{fr} values for the five scenarios are presented in Table 5 and illustrated in Figs. 11 and 12, respectively. Overall, at all depths, the case of sub-only setup showed the highest t_e and lowest T_{fr} values, whereas the main-main setup showed the lowest t_e and highest T_{fr} values among the five scenarios. The missing values of t_e for the sub-only case at 55.9 and 70.7 cm from the freezing pipe and the t_e values at 50 cm from the freezing pipe at the depths of 3 and 4 m indicate that a semi-spherical shape (or ovoid shape) of frozen soil was formed (no values at the depths of 2 and 5 m) with a radius of frozen mass of 50 cm. The t_e and T_{fr} values presented in Figs. 11 and 12 indicate that a single sub-freezing pipe can be utilized to form relatively small-sized frozen soil with a low freezing rate.

The semi-spherical shape of the formed frozen soil was induced by dominant heat extraction from the range of 3–4 m depth of the 5-m-long freezing pipe with thermal insulation up to 2 m. This led to the most dominant heat extraction in the vertical direction and the most rapid growth of frozen soil at the depths of 3 and 4 m.

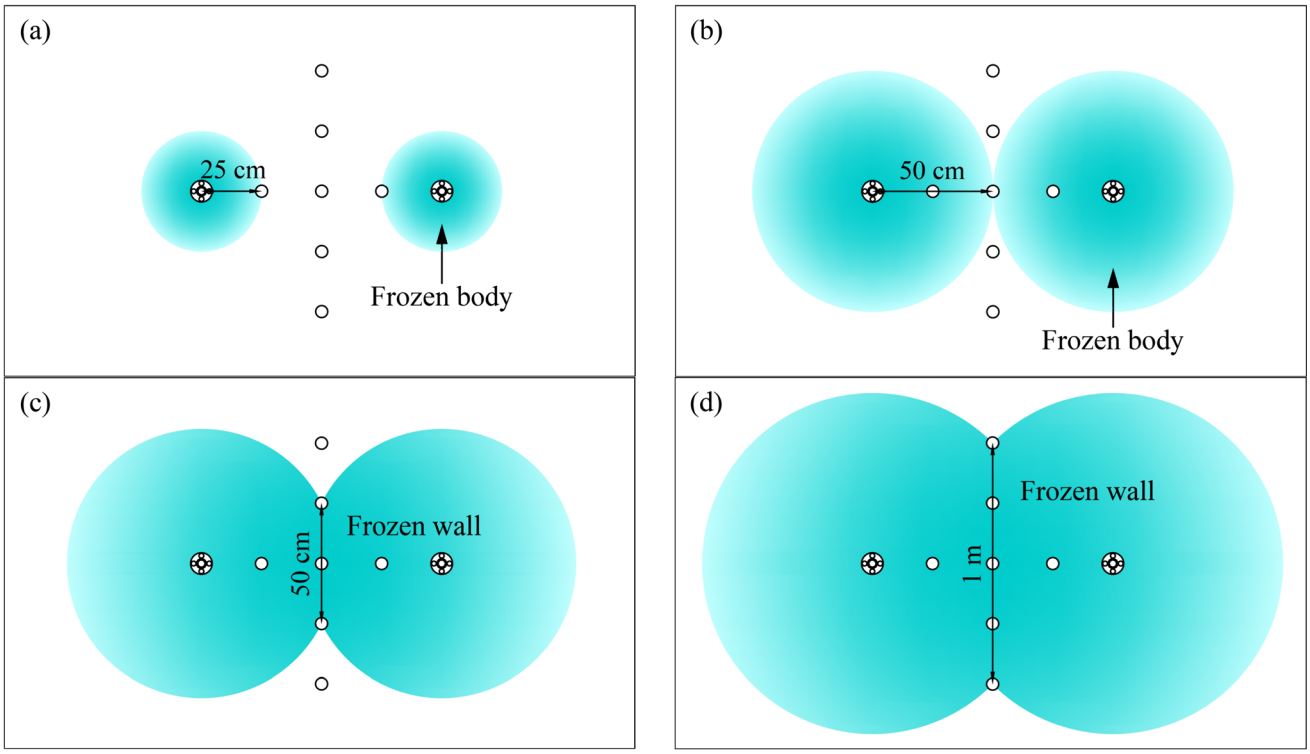

Fig. 10 Formation of frozen wall in four stages: **a** Stage 1, **b** Stage 2, **c** Stage 3, and **d** Stage 4

Table 5 t_e and T_{fr} values of all experimental conditions (corresponding to Figs. 11 and 12)

Depth (m)	t_e (days)					T_{fr} (days)				
	D = 25 cm					D = 25 cm				
	Sub only	Main only	Main-main	Sub-sub	Main-sub	Sub only	Main only	Main-main	Sub-sub	Main-sub
2	1.34	1.86	0.94	0.99	0.81	3.43	2.84	3.82	3.99	4.00
3	0.61	1.81	0.31	0.42	0.28	4.36	3.07	4.64	4.53	4.67
4	0.40	1.66	0.28	0.32	0.19	4.57	3.33	4.67	4.63	4.76
5	N/A	N/A	0.34	N/A	0.19	N/A	N/A	4.63	N/A	4.75
Depth (m)	D = 50 cm					D = 50 cm				
	Sub only	Main only	Main-main	Sub-sub	Main-sub	Sub only	Main only	Main-main	Sub-sub	Main-sub
2	1.93	N/A	1.80	1.96	2.94	1.93	N/A	2.98	2.07	0.99
3	1.94	1.96	0.84	1.81	1.59	1.96	2.18	4.17	3.16	3.40
4	1.04	1.82	0.65	1.34	1.33	3.97	3.01	4.31	3.61	3.61
5	N/A	N/A	0.93	N/A	1.62	N/A	N/A	4.05	N/A	3.27
Depth (m)	D = 55.9 cm					D = 55.9 cm				
	Sub only	Main only	Main-main	Sub-sub	Main-sub	Sub only	Main only	Main-main	Sub-sub	Main-sub
2	N/A	N/A	1.93	2.97	2.98	N/A	N/A	2.09	0.99	0.36
3	3.02	N/A	1.34	1.93	1.76	0.93	N/A	3.61	2.74	2.93
4	2.96	N/A	0.84	1.81	1.53	1.97	N/A	4.14	3.07	3.45
5	N/A	N/A	1.33	N/A	1.78	N/A	N/A	3.61	N/A	2.91
Depth (m)	D = 70.7 cm					D = 70.7 cm				
	Sub only	Main only	Main-main	Sub-sub	Main-sub	Sub only	Main only	Main-main	Sub-sub	Main-sub
2	N/A	N/A	3.01	N/A	N/A	N/A	N/A	0.38	N/A	N/A
3	N/A	N/A	1.84	2.99	3.02	N/A	N/A	3.07	1.28	0.93
4	4.65	N/A	1.61	2.96	2.96	0.38	N/A	3.37	1.99	1.97
5	N/A	N/A	1.93	N/A	N/A	N/A	N/A	2.84	N/A	N/A

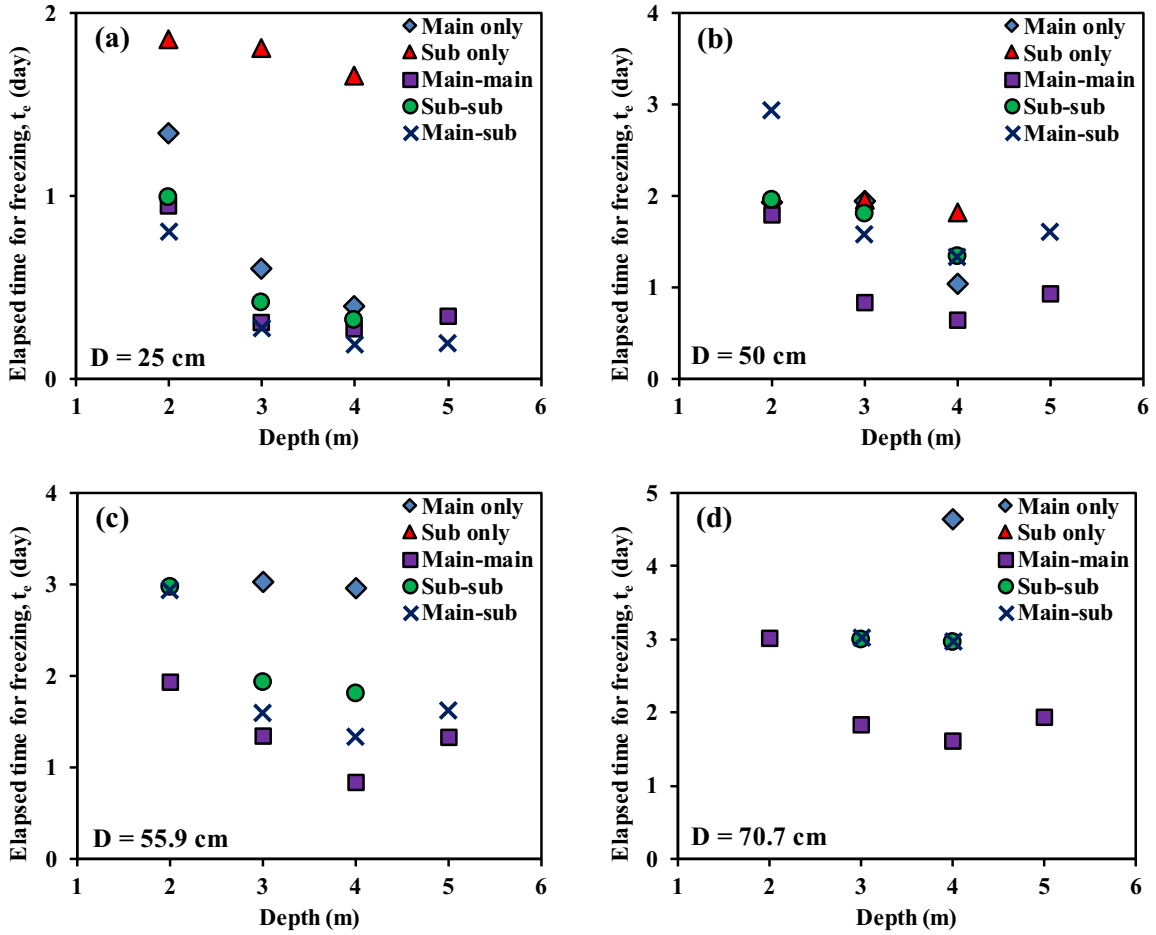

Fig. 11 Evaluated elapsed freezing time for five scenarios at a distance of **a** 25 cm, **b** 50 cm, **c** 55.9 cm, and **d** 70.7 cm from freezing pipe. The missing data represents above-zero temperature for 5 days of injection

3.4 Implications of experimental observations

Adopting liquid nitrogen provided rapid freezing with a sufficient increase in the strength and stiffness of soils. However, the high cost of liquid nitrogen limits the application of the open-system AGF [9, 16, 42]. Although liquid nitrogen can be reused after initial injection when the outlet temperature is below zero, no study investigated the reuse of liquid nitrogen for secondary injection in the AGF method.

The monitored temperatures presented in Figs. 5, 6, 7, 8, and 9 reveal the favorable applicability of reusing liquid nitrogen after the initial injection. The monitored temperatures around the two sub-freezing pipes and the main-sub freezing pipes also indicate the capability of forming a 1-m-thick frozen wall after 3 days by reusing liquid nitrogen. The relatively short required time (1.6 days for forming a 1-m-thick frozen wall) for the two main freezing pipes indicates that the typical practice of AGF using the first injection of liquid nitrogen only should be adopted in case of forming thick frozen walls in a short time. Nevertheless, because the target frozen wall thickness of 1 m is commonly adopted in AGF specifications for underground construction [14, 24, 29], the results presented in this study demonstrate the applicability of reusing liquid nitrogen for developing frozen walls for various construction projects.

The experimental observations presented in this study demonstrated the reusability of liquid nitrogen, though this is limited to saturated silty deposits. However, it's worth noting that AGF can be applied to soil deposits with a water content higher than 15% [22, 41], suggesting that liquid nitrogen could potentially be reused in many types of soil deposits located below the groundwater level. Previous studies reported that the rate of heat extraction in the freezing process depends on several factors, such as soil type [1, 15, 47], degree of ice saturation [51], configuration and material of freezing pipes [14, 29], pore water salinity [31, 49], flow rate and direction of groundwater [20, 27, 33], geochemical aspects [44], and injection rate [4]. Further investigations are required to assess the reuse of liquid nitrogen under various field conditions.

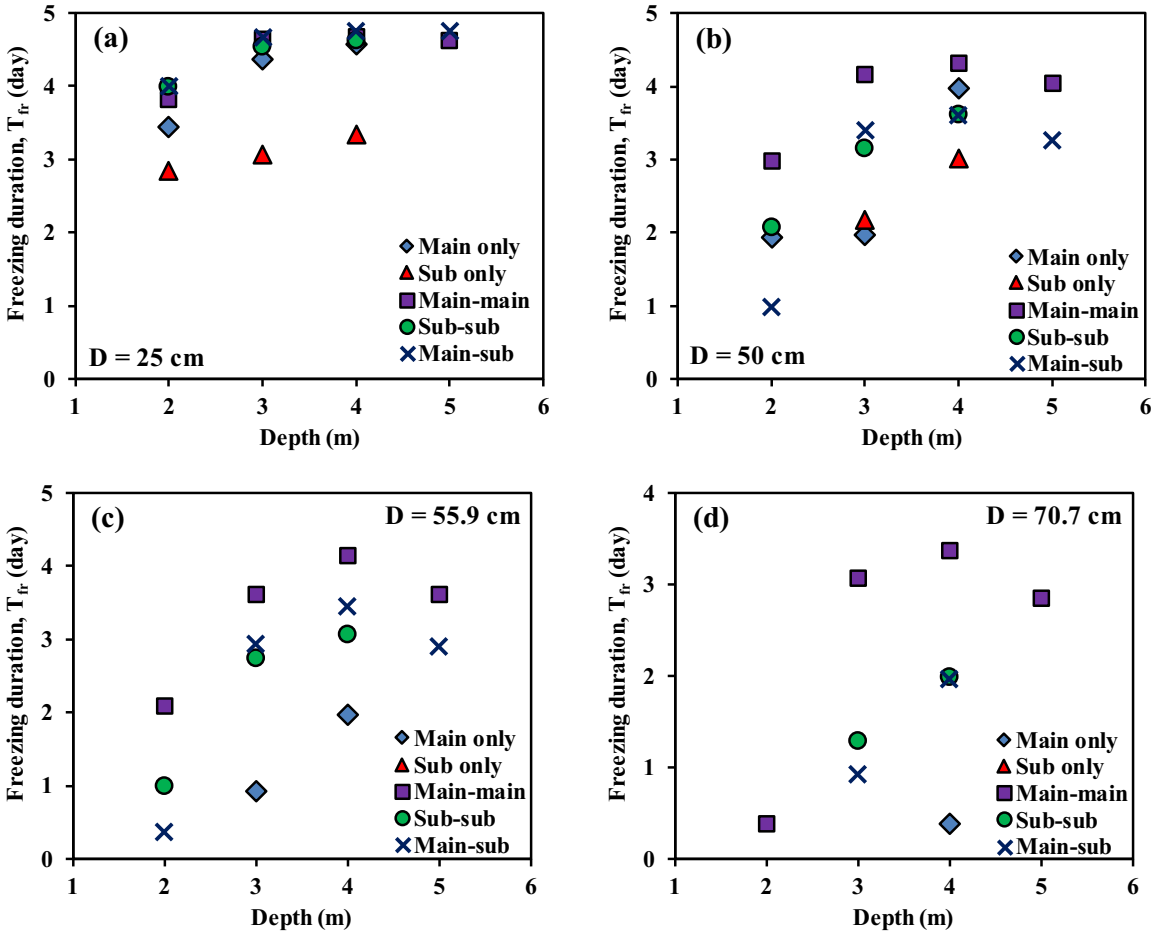

Fig. 12 Evaluated freezing duration for five scenarios at a distance of **a** 25 cm, **b** 50 cm, **c** 55.9 cm, and **d** 70.7 cm from freezing pipe. The missing data represents above-zero temperature for 5 days of injection

3.5 Cost estimation for forming 1-m-thick frozen wall between two freezing pipes

In this study, approximately 30% of cost reduction would be anticipated by reusing the liquid nitrogen. For example, the estimated costs to achieve D = 70.7 cm are approximately $2,715 for using only liquid nitrogen and $1928 for the scenario of reusing liquid nitrogen. This estimation assumed that the consumption of liquid nitrogen in the reusing scenario is half that of using liquid nitrogen only. The calculation was based on a unit price of liquid nitrogen at $200 per ton, the average t_e values in Table 5 for the main-main and sub-sub setups, and the daily consumption rate of 6.473 ton/day as indicated in Table 3. An even higher cost was estimated for the circulation of brine mainly because of the need for installing a freezing plant. The abovementioned calculation results imply significant cost benefits in AGF-related projects by reusing liquid nitrogen for forming a 1-m-thick frozen wall.

The accurate cost estimation of AGF projects is challenging and depends on many factors such as the number of freezing pipes, seepage flow, freezing duration, target freezing volume (or thickness), installation process, and transportation. Therefore, injecting liquid nitrogen into all freezing pipes might be more beneficial than reusing liquid nitrogen for the project with a high operational cost per day (e.g., labor) (reusing liquid nitrogen requires one or two days longer to form a 1-m-thick frozen wall compared with injecting liquid nitrogen). Nevertheless, the material-wise cost estimation indicates the reuse of liquid nitrogen is beneficial for large AGF-related projects, which require the installation of hundreds of freezing pipes. Note that the circulation of brine may be a cost-beneficial method for maintaining a frozen mass of soils for relatively long projects because of low material-related costs (cost without freezing plant).

4 Conclusion

This study investigated the reusability of liquid nitrogen by performing a field experiment under five scenarios: main-only, sub-only, main-main, sub-sub, and main-sub setups. The freezing of silty deposits near the freezing pipes (or between the two freezing pipes) was assessed from the monitored temperature up to the depth of 5 m. Additionally, the freezing rate, elapsed freezing time, and freezing duration were evaluated for quantitative representation and applicability of reusing liquid nitrogen after the initial injection. Based on the monitored temperature data at the temperature-measuring holes, freezing rate, elapsed freezing time, and freezing duration, the following conclusions were obtained:

1. The monitored temperature of − 120 °C at the depth of 5 m for the sub-freezing pipe indicates that the temperature of nitrogen after the initial injection was sufficiently low to freeze the surrounding soil.
2. The highest rate of heat extraction was observed at the main-main setup, while the lowest rate was observed at the sub-only setup. Additionally, a similar rate of heat extraction for the main-only and sub-sub setups indicates the efficiency of additional sub-freezing pipes in the formation of the frozen soil.
3. The sub-zero temperatures observed at the temperature-measuring hole that is located between two sub-freezing pipes implies that a 1-m-thick frozen wall can be formed by injecting reused liquid nitrogen into the two adjacent sub-freezing pipes with 1 m interval.
4. The observed temperature data at the temperature-measuring holes, one-dimensional freezing rate in the radial direction, elapsed freezing time, and freezing duration indicates the applicability of reusing liquid nitrogen in silty deposits. Further investigations are required to verify the efficiency of reusing liquid nitrogen under various hydrogeological conditions and the arrangement of freezing pipes.
5. The results presented in this study suggest a significant potential for reusing liquid nitrogen on construction sites, which could substantially reduce the cost of AGF. Traditionally, AGF using liquid nitrogen without reuse has been regarded as one of the high-cost ground improvement methods.

Acknowledgements This research was supported by the National Research Foundation of Korea (NRF) Grants funded by the Korean government (No. RS-2023-00221719) and Korea Agency for Infrastructure Technology Advancement under the Ministry of Land, Infrastructure and Transport (No. RS-2024-00410248).

Data availability The data used in this study are available from the corresponding author (jwon@unist.ac.kr) upon request.

References

1. Alzoubi MA, Nie-Rouquette A, Ghoreishi-Madiseh SA et al (2019) On the concept of the freezing-on-demand (FoD) in artificial ground freezing for long-term applications. Int J Heat Mass Transf 143:118557. https://doi.org/10.1016/j.ijheatmasstransfer.2019.118557
2. Alzoubi MA, Nie-Rouquette A, Sasmito AP (2018) Conjugate heat transfer in artificial ground freezing using enthalpy-porosity method: experiments and model validation. Int J Heat Mass Transf 126:740–752. https://doi.org/10.1016/j.ijheatmasstransfer.2018.05.059
3. Alzoubi MA, Poncet S, Sasmito AP (2021) Hybrid artificial ground freezing as a sustainable solution for containing hazardous-waste in critical environmental projects. Cold Reg Sci Technol 192:103401. https://doi.org/10.1016/j.coldregions.2021.103401
4. Alzoubi MA, Sasmito AP, Madiseh A, Hassani FP (2017) Intermittent freezing concept for energy saving in artificial ground freezing systems. Energy Procedia 142:3920–3925. https://doi.org/10.1016/j.egypro.2017.12.297
5. Andersland OB, Ladanyi B (2013) An introduction to frozen ground engineering. Springer, New York
6. Andersland OB, Wiggert DC, Davies SH (1996) Hydraulic conductivity of frozen granular soils. J Environ Eng 122:212–216. https://doi.org/10.1061/(ASCE)0733-9372(1996)122:3(212)
7. Becker BR, Misra A, Fricke BA (1992) Development of correlations for soil thermal conductivity. Int Commun Heat Mass Transf 19:59–68. https://doi.org/10.1016/0735-1933(92)90064-O
8. Bing H, Ma W (2011) Laboratory investigation of the freezing point of saline soil. Cold Reg Sci Technol 67:79–88. https://doi.org/10.1016/j.coldregions.2011.02.008
9. Braun B, Shuster J, Burnham E (1979) Ground freezing for support of open excavations. Eng Geol 13:429–453. https://doi.org/10.1016/0013-7952(79)90048-6
10. Casini F, Gens A, Olivella S, Viggiani GMB (2016) Artificial ground freezing of a volcanic ash: laboratory tests and modelling. Environ Geotech 3:141–154. https://doi.org/10.1680/envgeo.14.00004
11. Casini F, Guida G, Restaini A, Celot A (2023) Water retention curve-based design method for the artificial ground freezing: the Isarco river underpass tunnels within the brenner base tunnel project. J Geotech Geoenviron Eng. https://doi.org/10.1061/JGGEFK.GTENG-10723
12. Cavuoto F, Manassero V, Russo G, Corbo A (2020) Urban tunnelling under archaeological findings in Naples (Italy) with ground freezing and grouting techniques. Tunnels and underground cities. Engineering and innovation meet archaeology, architecture and art. CRC Press, New York, pp 32–41
13. Choi H-J, Won J, Lee D et al (2021) Effect of ground freezing with liquid nitrogen on freezing rate and mechanical properties of coastal clayey silt. J Eng Mech 147:04021057. https://doi.org/10.1061/(asce)em.1943-7889.0001974
14. Crippa C, Manassero V (2006) Artificial ground freezing at sophiaspoortunnel (The Netherlands)—Freezing parameters: data acquisition and processing. In: GeoCongress 2006: Geotechnical engineering in the information technology age. pp 1–6
15. Evirgen B, Tuncan M (2019) A physical soil freezing model for laboratory applications. Cold Reg Sci Technol 159:29–39. https://doi.org/10.1016/j.coldregions.2018.12.005
16. Fan W, Yang P, Yang Z, (Joey), (2019) Impact of freeze-thaw on the physical properties and compressibility of saturated clay. Cold Reg Sci Technol 168:102873. https://doi.org/10.1016/j.coldregions.2019.102873

17. He H, Flerchinger GN, Kojima Y et al (2021) A review and evaluation of 39 thermal conductivity models for frozen soils. Geoderma 382:114694. https://doi.org/10.1016/j.geoderma.2020.114694
18. Hu X, Han L, Han Y (2019) Analytical solution to temperature distribution of frozen soil wall by multi-row-piped freezing with the boundary separation method. Appl Therm Eng 149:702–711. https://doi.org/10.1016/j.applthermaleng.2018.12.096
19. Hu R, Liu Q, Xing Y (2018) Case study of heat transfer during artificial ground freezing with groundwater flow. Water 10:1322. https://doi.org/10.3390/w10101322
20. Huang S, Guo Y, Liu Y et al (2018) Study on the influence of water flow on temperature around freeze pipes and its distribution optimization during artificial ground freezing. Appl Therm Eng 135:435–445. https://doi.org/10.1016/j.applthermaleng.2018.02.090
21. Jessberger HL (2017) A state-of-the-art report. Ground freezing: Mechanical properties, processes and design. In: Ground Freezing 1980: Selected Papers from the Second International Symposium on Ground Freezing, Trondheim, Norway, Elsevier, Amsterdam, p 5
22. Jones JS, Brown RE (1979) Design of tunnel support systems using ground freezing. Eng Geol 13:375–395. https://doi.org/10.1016/0013-7952(79)90044-9
23. Kang Y, Hou C, Li K et al (2021) Evolution of temperature field and frozen wall in sandy cobble stratum using LN2 freezing method. Appl Therm Eng 185:116334. https://doi.org/10.1016/j.applthermaleng.2020.116334
24. Konrad J-M (2002) Prediction of freezing-induced movements for an underground construction project in Japan. Can Geotech J 39:1231–1242. https://doi.org/10.1139/t02-077
25. Kurz D, Alfaro M, Graham J (2017) Thermal conductivities of frozen and unfrozen soils at three project sites in northern Manitoba. Cold Reg Sci Technol 140:30–38. https://doi.org/10.1016/j.coldregions.2017.04.007
26. Levin L, Golovatyi I, Zaitsev A et al (2021) Thermal monitoring of frozen wall thawing after artificial ground freezing: case study of Petrikov Potash Mine. Tunn Undergr Sp Technol 107:103685. https://doi.org/10.1016/j.tust.2020.103685
27. Li Z, Chen J, Sugimoto M, Ge H (2019) Numerical simulation model of artificial ground freezing for tunneling under seepage flow conditions. Tunn Undergr Sp Technol 92:103035. https://doi.org/10.1016/j.tust.2019.103035
28. Li J, Tang Y, Feng W (2020) Creep behavior of soft clay subjected to artificial freeze–thaw from multiple-scale perspectives. Acta Geotech 15:2849–2864. https://doi.org/10.1007/s11440-020-00980-2
29. Li D, Wang H (2010) Investigation into artificial ground freezing technique for a cross passage in metro. In: Deep and underground excavations. pp 294–299
30. Liu Y, Li K-Q, Li D-Q et al (2022) Coupled thermal–hydraulic modeling of artificial ground freezing with uncertainties in pipe inclination and thermal conductivity. Acta Geotech 17:257–274. https://doi.org/10.1007/s11440-021-01221-w
31. Lyu C, Nishimura S, Amiri SAG et al (2021) Pore-water pressure development in a frozen saline clay under isotropic loading and undrained shearing. Acta Geotech 16:3831–3847. https://doi.org/10.1007/s11440-021-01338-y
32. Manassero V, Di Salvo G, Giannelli F, Colombo G (2008) A combination of artificial ground freezing and grouting for the excavation of a large size tunnel below groundwater
33. Marwan A, Zhou M-M, Zaki Abdelrehim M, Meschke G (2016) Optimization of artificial ground freezing in tunneling in the presence of seepage flow. Comput Geotech 75:112–125. https://doi.org/10.1016/j.compgeo.2016.01.004
34. Massarotti N, Mauro A, Normino G, et al (2019) Thermal phenomena model for artificial ground freezing during a tunnel excavation for the Municipio Metro station in Naples, Italy. In: Tunnels and underground cities: engineering and innovation meet archaeology, architecture and art. CRC Press, pp 1409–1418
35. Nicotera MV, Russo G (2021) Monitoring a deep excavation in pyroclastic soil and soft rock. Tunn Undergr Sp Technol 117:104130. https://doi.org/10.1016/j.tust.2021.104130
36. Nikolaev P, Shuplik M (2019) Low-temperature ground freezing methods for underground construction in urban areas. In: MATEC Web of Conferences. EDP Sciences, p 4020
37. Penner E (1970) Thermal conductivity of frozen soils. Can J Earth Sci 7:982–987. https://doi.org/10.1139/e70-091
38. Pimentel E, Papakonstantinou S, Anagnostou G (2012) Numerical interpretation of temperature distributions from three ground freezing applications in urban tunnelling. Tunn Undergr Sp Technol 28:57–69. https://doi.org/10.1016/j.tust.2011.09.005
39. Russo G, Cavuoto F, Corbo A, Manassero V (2022) Municipio Station Metro Line 6 in Naples: a case of urban tunnelling adopting ground freezing and grouting techniques to underpass archaeological findings. In: Geotechnical Engineering for the Preservation of Monuments and Historic Sites III. CRC Press, New York, pp 937–950
40. Russo G, Corbo A, Cavuoto F, Autuori S (2015) Artificial ground freezing to excavate a tunnel in sandy soil. Measurements and back analysis. Tunn Undergr Sp Technol 50:226–238. https://doi.org/10.1016/j.tust.2015.07.008
41. Shuster JA (1981) Engineering quality assurance for construction ground freezing. Eng Geol 18:333–350. https://doi.org/10.1016/0013-7952(81)90072-7
42. Stille B, Brantmark J, Wilson L, Håkansson U (2017) Ground freezing design in tunnelling–Two case studies from Stockholm. In: Tunnels and underground structures. Routledge, New York, pp 185–190
43. Tian Z, Lu Y, Horton R, Ren T (2016) A simplified de Vries-based model to estimate thermal conductivity of unfrozen and frozen soil. Eur J Soil Sci 67:564–572. https://doi.org/10.1111/ejss.12366
44. Tounsi H, Rouabhi A, Jahangir E (2020) Thermo-hydro-mechanical modeling of artificial ground freezing taking into account the salinity of the saturating fluid. Comput Geotech 119:103382. https://doi.org/10.1016/j.compgeo.2019.103382
45. Tounsi H, Rouabhi A, Tijani M, Guérin F (2019) Thermo-hydro-mechanical modeling of artificial ground freezing: application in mining engineering. Rock Mech Rock Eng 52:3889–3907. https://doi.org/10.1007/s00603-019-01786-9
46. Vitel M, Rouabhi A, Tijani M, Guérin F (2015) Modeling heat transfer between a freeze pipe and the surrounding ground during artificial ground freezing activities. Comput Geotech 63:99–111. https://doi.org/10.1016/j.compgeo.2014.08.004
47. Vu QH, Pereira J-M, Tang AM (2022) Effect of fines content on soil freezing characteristic curve of sandy soils. Acta Geotech. https://doi.org/10.1007/s11440-022-01672-9
48. Wang B, Rong C, Lin J et al (2019) Study on the formation law of the freezing temperature field of freezing shaft sinking under the action of large-flow-rate groundwater. Adv Mater Sci Eng 2019:1–20. https://doi.org/10.1155/2019/1670820
49. Wang S, Wang Q, Qi J, Liu F (2018) Experimental study on freezing point of saline soft clay after freeze-thaw cycling. Geomech Eng 15:997–1004
50. Won J, Lee D, Choi H-J et al (2022) Field experiments for three freezing operation scenarios in silty soil deposits. Eng Geol 303:106642. https://doi.org/10.1016/j.enggeo.2022.106642
51. Zhou M-M, Meschke G (2018) A multiscale homogenization model for strength predictions of fully and partially frozen soils.

Acta Geotech 13:175–193. https://doi.org/10.1007/s11440-017-0538-0